THE JOURNAL OF BIOLOGICAL CHEMISTRY VOL. 284, NO. 13, pp. 8621–8632, March 27, 2009

Poly(ADP-ribose) Polymerase 1 Interacts with Nuclear Respiratory Factor 1 (NRF-1) and Plays a Role in NRF-1 Transcriptional Regulation*[S]

Received for publication, September 17, 2008, and in revised form, January 7, 2009 Published, JBC Papers in Press, January 30, 2009, DOI 10.1074/jbc.M807198200

Mohammad B. Hossain, Ping Ji, Ramakrishnan Anish, Raymond H. Jacobson, and Shinako Takada[1]

From the Department of Biochemistry and Molecular Biology, Genes and Development Program of the Graduate School of Biomedical Sciences, The University of Texas M. D. Anderson Cancer Center, Houston, Texas 77030

Nuclear respiratory factor 1 (NRF-1) is one of the key transcriptional activators for nuclear-coded genes involved in mitochondrial biogenesis and function as well as for many housekeeping genes. A transcriptional co-activator PGC-1 and its related family member PRC have previously been shown to interact with NRF-1 and co-activate NRF-1. We show here that NRF-1 can also directly interact with poly(ADP-ribose) polymerase 1 (PARP-1) and co-purify the PARP-1·DNA-PK·Ku80·Ku70·topoisomerase IIβ-containing protein complex. Our *in vitro* binding experiments show that DNA-binding/dimerization domain of NRF-1 and the N-terminal half of PARP-1, which contains two Zinc fingers and the auto-modification domain, are responsible for the interaction, and that this interaction occurs with or without PARP-1 poly(ADP-ribosyl)ation (PARylation). DNA-bound NRF-1 can form a complex with PARP-1, suggesting that NRF-1 can recruit the PARP-1·DNA-PK·Ku80·Ku70·topoisomerase IIβ-containing protein complex to the promoter. PARP-1 can also PARylate the DNA-binding domain of NRF-1 and negatively regulate NRF-1·PARP-1 interaction. Transient transfection and chromatin immunoprecipitation experiments suggest that PARP-1 plays a role during transcriptional activation by NRF-1. Our finding identifies a new aspect of transcriptional regulation used by NRF-1.

Nuclear respiratory factor 1 (NRF-1)[2] is a DNA-binding transcription factor that activates genes that are involved in mitochondrial biogenesis and function and other fundamental cellular functions, such as protein translation/turnover, DNA synthesis/repair, and cell proliferation (see Refs. 1 and 2 for review). NRF-1 binds sequence-specifically to a GC-rich DNA element (RCGCRYGCGY). Early studies showed that this DNA sequence motif was mostly found in TATA-less promoters (3). A recent bioinformatics study further showed that the NRF-1-binding motif is one of the seven over-represented DNA sequences in the human genome present at core promoters (*i.e.* 40–50 bp DNA regions around transcriptional start sites) (4). Taken together, NRF-1 appears to be involved in transcription from a large number of TATA-less promoters and to often play a role as a proximal promoter-binding factor.

Previous studies have identified several important co-factors that interact with NRF-1, including the transcriptional co-activators PGC (PPARγ co-activator)-1α, PGC-1β, and PRC (PGC-1-related co-activator) (5–7). PGC-1α has been shown to interact with the DNA-binding/dimerization domain of NRF-1 (6). PGC-1α has also been shown to interact with other nuclear factors including RNA polymerase II, the transcriptional mediator complex, histone acetyltransferases SRC-1 and p300, and an RNA splicing factor (8–10). These findings suggest mechanisms that NRF-1 may utilize to activate transcription. First, NRF-1 may accelerate recruitment of RNA polymerase II to the promoter region through bridging interactions mediated by PGC-1. Second, NRF-1 transcriptional activation may involve changing local chromatin structure by recruitment of histone acetyltransferases via interactions with PGC-1.

However, a number of questions remain to be addressed, regarding the mechanisms of transcriptional activation by NRF-1. Expression of known NRF-1 co-activators is induced only when a high level of mitochondrial function or mitochondrial biogenesis (and therefore a high level of NRF-1 activity) is transiently required. For example, induction of PGC-1α expression occurs in response to cold exposure, fasting, exercise (for muscle cells), etc., and PRC is expressed in the immediately early phase after growth stimulation. PGC-1β appears to show a similar expression pattern to that of PGC-1α. However, it is unclear whether or what other co-factor(s) maintain expression of NRF-1 target genes when expression of the known PGC-1 family members is not induced. Other than the PGC-1 family members, dynein light chain has been reported to interact with the first 26 amino acids of NRF-1 (11), but the role of dynein light chain in transcriptional regulation by NRF-1 is still unclear. NRF-1 has also a transcriptional activation domain that was defined using Gal4 DNA-binding domain fusions (12). However, this activation domain contains no amino acid

* This work was supported, in whole or in part, by National Institutes of Health Grant AI057504 (to S. T.) and GM069769 (to R. J.). This work was also supported by the DNA core facility at the M. D. Anderson Cancer Center. The costs of publication of this article were defrayed in part by the payment of page charges. This article must therefore be hereby marked "*advertisement*" in accordance with 18 U.S.C. Section 1734 solely to indicate this fact.

[S] The on-line version of this article (available at http://www.jbc.org) contains supplemental Fig. S1.

[1] To whom correspondence should be addressed: Unit 1000, 1515 Holcombe Blvd., Houston TX 77030. Tel.: 713-834-6275; Fax: 713-834-6266; E-mail: stakada@mdanderson.org.

[2] The abbreviations used are: NRF, nuclear respiratory factor; PARP, poly(ADP-ribose) polymerase; DNA-PK, DNA-dependent protein kinase; Topo, topoisomerase; PARylation, poly(ADP-ribosyl)ation; HBV, hepatitis B virus; GST, glutathione *S*-transferase; CBP, calmodulin-binding peptide; EMSA, electrophoretic mobility shift assay; Ni-NTA, nickel-nitrilotriacetic acid; aa, amino acid(s); MEF, mouse embryonic fibroblast; siRNA, small interfering RNA; ChIP, chromatin immunoprecipitation; RT, reverse transcription; PIPES, 1,4-piperazinediethanesulfonic acid.

sequence motifs previously found in other transcriptional activation domains, nor has an interacting partner for this domain been identified. Therefore, it appeared there was a need to identify more factors that interact with NRF-1.

We previously found that NRF-1 binds to the hepatitis B virus (HBV) X gene promoter and positively regulates X gene transcription (13). Further analyses of the X promoter structure showed that the X mRNA displayed two major transcriptional start sites (start site 1 and start site 2), and transcription from these start sites was individually driven by two independent core promoters. The core promoter for Start site 1 contains two essential DNA elements for its core promoter activity, a NRF-1-binding site and a novel core promoter element XCPE1. We have shown that transcription from Start site 1 is dependent on NRF-1 function (14).

To better understand the role of NRF-1 during transcription of the HBV X gene and other cellular NRF-1 target genes, we screened crude nuclear extracts to identify NRF-1-interacting proteins. We report here a novel interaction between NRF-1 and a poly(ADP-ribose) polymerase 1 (PARP-1)·DNA-PK·Ku80·Ku70·topoisomerase IIβ (TopoIIβ)-containing complex mediated through a direct interaction with PARP-1. Our results suggest NRF-1 can activate transcription by enhancing recruitment of RNA polymerase II via a protein-protein interaction pathway between NRF-1-PARP-1-mediator-RNA polymerase II and/or by using enzymatic activities of PARP-1·DNA-PK·Ku80·Ku70·TopoIIβ-containing complex. Our results identify a novel pathway utilizing a PARP-1 complex that may be used by NRF-1 to activate transcription from a large class of TATA-less promoters.

EXPERIMENTAL PROCEDURES

Plasmids, Recombinant Protein Expression, and Purification—For the N-terminally FLAG-tagged NRF-1, NRF-1 cDNA was cloned into a modified pAcSG2 vector (PharMingen) and co-transfected into SF9 cells with BaculoGold DNA (PharMingen). To express N-terminally His-tagged NRF-1 in *Escherichia coli*, NRF-1 cDNA was cloned into pET19b (Novagen). The bacterial expression plasmid for untagged full-length NRF-1 (3) was a generous gift from Richard Scarpulla. Bacterial expression plasmids for the N-terminally GST-fused NRF-1 (full-length and deletion mutants) were constructed using the Gateway system (Invitrogen). For preparation of the untagged NRF-1 DNA-binding domain, a TEV protease recognition site was introduced between the GST and the NRF-1 domain. The NRF-1 DNA-binding domain protein was purified by glutathione-Sepharose affinity chromatography, cleavage of the NRF-1 DNA-binding domain from GST tag by TEV protease, and then further purified using ion exchange chromatography. The NRF-1 eukaryotic expression plasmid pSG5-NRF-1 was from Richard Scarpulla as previously described (13).

For expression of full-length His- or GST-tagged PARP-1, a baculovirus system (Bac-to-bac system; Invitrogen) was used. The PARP-1 proteins were affinity-purified and then further fast protein liquid chromatography-purified as needed. PARP-1 mutant proteins were expressed as untagged forms using the Bac-to-bac system. The N-terminal 650 amino acids of PARP-1 were recoded to produce a "synthetic PARP-1" gene and cloned into pET-Duet vector (Novagen) as a calmodulin-binding peptide (CBP) fusion for efficient bacterial expression. The bacterial expression plasmid for seven other PARP-1 deletion mutants were also constructed from the synthetic PARP-1 gene and expressed in *E. coli* as GST fusions. The PARP-1 eukaryotic expression plasmid was driven by a CMV promoter.

A human cytochrome *c* promoter reporter plasmid was constructed by PCR cloning the promoter region (from −993 to +56 relative to the transcriptional start site) from genomic DNA and inserting it to pGL2-basic (Promega). A cytochrome *c* reporter plasmid with a mutation at the NRF-1-binding site located between −169 and −154 relative to the major transcriptional start site was constructed by the QuikChange method (Stratagene).

Identification of NRF-1-interacting Proteins—Baculovirally expressed N-terminally FLAG-tagged NRF-1 was immunopurified by anti-FLAG (M2) antibody beads (Sigma). The resultant beads were incubated with nuclear extracts from either HepG2 or HeLa cells. The bound fractions were extensively washed and analyzed by SDS-PAGE. To prevent detection of false-positive proteins through DNA-mediated interactions, the beads were treated with DNase I before and after the pull-down. Silver-stained bands of the specifically bound proteins were excised from the polyacrylamide gel, destained, and digested in-gel using Trypsin Gold (Promega). Digested peptides were extracted as described in Promega technical bulletin (TB309) and separated on a Vydac Everest C18 reversed phase column using acetonitrile/water gradient in the presence of 0.1% formic acid. Eluent from the C18 column was directly applied to an Agilent LC-MSD electrospray ion trap MS/MS spectrometer. Fragmentation spectra were collected and analyzed using MASCOT (Matrix Biosciences). Proteins with significant identity were reported.

Antibodies—Rabbit anti-human NRF-1 antibody used for Western blotting was generated by immunizing rabbits with an N-terminally His-tagged full-length NRF-1 that was expressed and purified from bacteria. Chicken anti-human NRF-1 was generated by immunizing chickens with the full-length untagged NRF-1 that was bacterially expressed and purified as described (3). To immunoprecipitate NRF-1 with chicken anti-NRF-1 antibody, PrecipiHen (agarose-coupled goat anti-chicken IgY; Aves Lab) was used. Anti-PARP-1 was generated by immunizing rabbits with an N-terminally His-tagged full-length PARP-1 that was expressed and purified as described above. Anti-PARP-1 antibody was affinity-purified by an Affi-Gel affinity column that was cross-linked to the CBP-fused synthetic PARP-1. Anti-DNA-PK and anti-TopoIIβ were purchased from Bethyl Laboratories, Inc. Anti-Ku80 and anti-Ku70 were from Santa Cruz Biotechnology. Anti-poly(ADP-ribose) (anti-PAR) was from Trevigen.

Electrophoretic Mobility Shift Assay (EMSA)—EMSA was performed using the 16-bp DNA fragment (MP4) from the HBV X promoter that contains the NRF-1-binding site (13). ^{32}P-Labeled MP4 DNA was incubated with proteins indicated in Fig. 4. The buffer for the protein-DNA binding reaction contained 20 mM Hepes (pH 7.9), 5% glycerol, 60 mM NaCl. After incubation at 30 °C for 30 min, the binding reaction was analyzed by PAGE (4% acrylamide gel, Tris/glycine/EDTA buffer, pH 8.8) followed by autoradiography.

PARylation Experiments—To auto-PARylate PARP-1, the purified His-tagged full-length PARP-1 protein on the Ni-NTA beads was incubated for 30 min at 30 °C in a PARylation buffer containing 20 mM Tris (pH 7.9), 100 mM NaCl, 10 mM $MgCl_2$, 10 μM $ZnCl_2$, 10% glycerol, 300 μM NAD^+, 1 mM dithiothreitol, 100 μg/ml sonicated salmon sperm DNA. To examine NRF-1 binding activity of auto-PARylated PARP-1, the Ni-NTA beads with the PARylated PARP-1 was washed once, the PARP-1 was eluted from the beads with the buffer containing 100 mM imidazole, 200 mM NaCl, 20 mM Tris (pH 7.9), 10% glycerol, 2 μM $ZnCl_2$, 1 mM dithiothreitol and then mixed with purified FLAG-NRF-1 immobilized on anti-FLAG (M2) beads.

To examine PARylation of NRF-1, purified His-PARP-1 or GST-PARP-1 (40 ng) was mixed with 400 ng of purified full-length no tag NRF-1, NRF-1 DNA-binding domain (aa 73–384), or other known or potential PARP-1 target proteins in the PARylation buffer described above in a 20-μl reaction at room temperature for 40 min and then examined for PARylation by Western blotting using anti-PAR antibody. For positive controls, purified p53 (Active Motif) and purified histones (Millipore) were used as PARylation substrates.

Transfection Experiments—HepG2 cells, HeLa cells, and *PARP-1*$^{-/-}$ mouse embryonic fibroblast (MEF) cells (15) were cultured in Dulbecco's modified Eagle's medium containing 10% fetal bovine serum. For transfection, Dharmafect Duo (Dharmacon) was used. One or 2 days after transfection, the cells were harvested, and RNA expression, protein expression, and the luciferase reporter activity were examined. For analysis of endogenous mRNAs, total RNA was isolated, and conventional RT-PCR or quantitative RT-PCR using Power SYBR Green RNA-to-CT 2-Step Kit (Applied Biosystems) was carried out. Double-stranded RNAs for siRNA experiments were purchased from Ambion (predesigned siRNA Select). PARP-1 inhibitors 4-amino-1,8-naphthalimide and 6(5H)-phenanthridinone were purchased from Trevigen.

Chromatin Immunoprecipitation (ChIP) Assay—HepG2 cells (~3×10^7) were cross-linked with 1.5 mM of a protein-protein cross-linker Ethylene glycolbis (succinimidyl succinate) (Pierce) at room temperature for 20 min (16) and with 1% formaldehyde at room temperature for 10 min. After stopping the cross-linking with 125 mM glycine, the cells were sedimented, washed, homogenized in cell lysis buffer (5 mM PIPES, 85 mM KCl, 0.5% Nonidet P-40, protease inhibitors). The nuclei were isolated by centrifugation and were resuspended in nuclei lysis buffer (50 mM Tris-HCl, 10 mM EDTA, 1% SDS). The nuclear lysates were sonicated to shear the DNA to a size range of ~100–500 bp. After centrifugation, the supernatant was diluted, precleared with PrecipiHen or protein A-Sepharose beads (Amersham Biosciences), preabsorbed with 20 mg/ml yeast RNA, 10 mg/ml salmon sperm DNA, and 10 mg/ml bovine serum albumin for 30 min, and then incubated with antiserum specific for NRF-1 or PARP-1 overnight. The immunocomplexes were collected with preabsorbed PrecipiHen (for NRF-1) or protein A-Sepharose beads (for PARP-1), the beads were extensively washed using different salt buffers. The immunocomplexes were eluted from beads with an elution buffer (0.1 M $NaHCO_3$, 1% SDS). The eluted complexes were incubated at 65 °C overnight to reverse the cross-link, and DNA was extracted by RNase A treatment, proteinase K digestion, phenol chloroform extraction, and ethanol precipitation and solubilized in water (~1.5×10^7 cell equivalent/100 μl). Cytochrome *c* promoter DNA fragments were detected by PCR using the following primers: 5′-CCGTACACCCTAACATGCTC-3′ and 5′-TGGCACAACGAACACTCC-3′ for amplifying −190 to +50; 5′-GCGTGTCCTTGGACTTAGAGA-3′ and 5′-CACAGCTCTGCCTCTAACCA-3′ for amplifying −14 to +110; and 5′-GGAGTGAAGACCCTGGACTG-3′ and 5′-CTTCAGCAACCACTACGGAA-3′ for amplifying +188 to +349. The DNA samples were heated to 98 °C for 30s, followed by 35 cycles of heating 98 °C for 10 s, annealing at 65 or 62 °C for 20 s, and extension at 72 °C for 10 s.

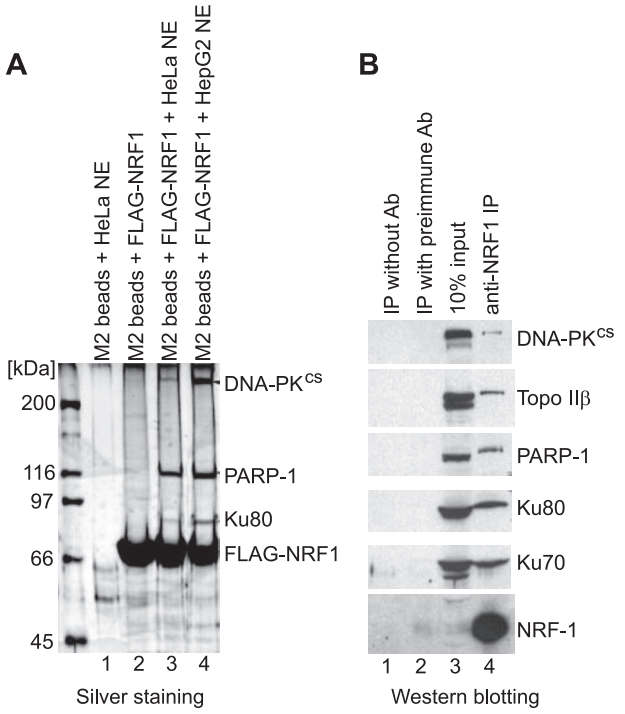

FIGURE 1. **NRF-1 co-purifies with a PARP-1·DNA-PK·Ku80·Ku70·TopoIIβ-containing complex.** *A*, isolation of NRF-1-interacting proteins. Approximately 1 μg of purified FLAG-NRF-1 on M2 beads was incubated with 10 mg of HepG2 or HeLa cell nuclear extract for 2 h at 4 °C and then washed five times with a washing buffer (20 mM Tris-HCl, pH 8.0, 0.25 M NaCl, 10% glycerol, 0.1% Nonidet P-40). The NRF-1-bound fractions (*lanes 3* and *4*) as well as the purified FLAG-NRF-1 alone on beads (*lane 2*) and the M2 beads incubated with HeLa nuclear extract in the absence of FLAG-NRF-1 (*lane 1*) were analyzed by SDS-PAGE (8% acrylamide) visualized by silver staining. *B*, the PARP-1·DNA-PK·Ku80·Ku70·TopoIIβ complex co-immunoprecipitates with NRF-1. HeLa nuclear extract (~500 μg) was precleared with the secondary antibody beads (agarose-coupled goat anti-chicken IgY) for 1 h, incubated with chicken anti-NRF-1 antibody at 4 °C overnight, and then mixed with the goat anti-chicken IgY beads for 1 h. Then the beads with the anti-NRF-1 immunocomplex were spun-down and washed three times with 25 mM Hepes (pH 7.9), 20% glycerol, 100 mM KCl, 2 mM $MgCl_2$, 0.2 mM EDTA three times. The washed beads were analyzed by Western blotting using the indicated primary antibodies. *IP*, immunoprecipitation.

RESULTS

NRF-1 Co-purifies with the PARP-1·DNA-PK·Ku80·Ku70·TopoIIβ Complex—To isolate NRF-1-interacting proteins, purified FLAG-NRF-1 protein was immobilized on beads and incubated with crude nuclear extracts from HepG2 or HeLa cells. Three proteins were found to be specifically bound to NRF-1 (Fig. 1*A*, *lanes 3* and *4*). These bands were isolated and

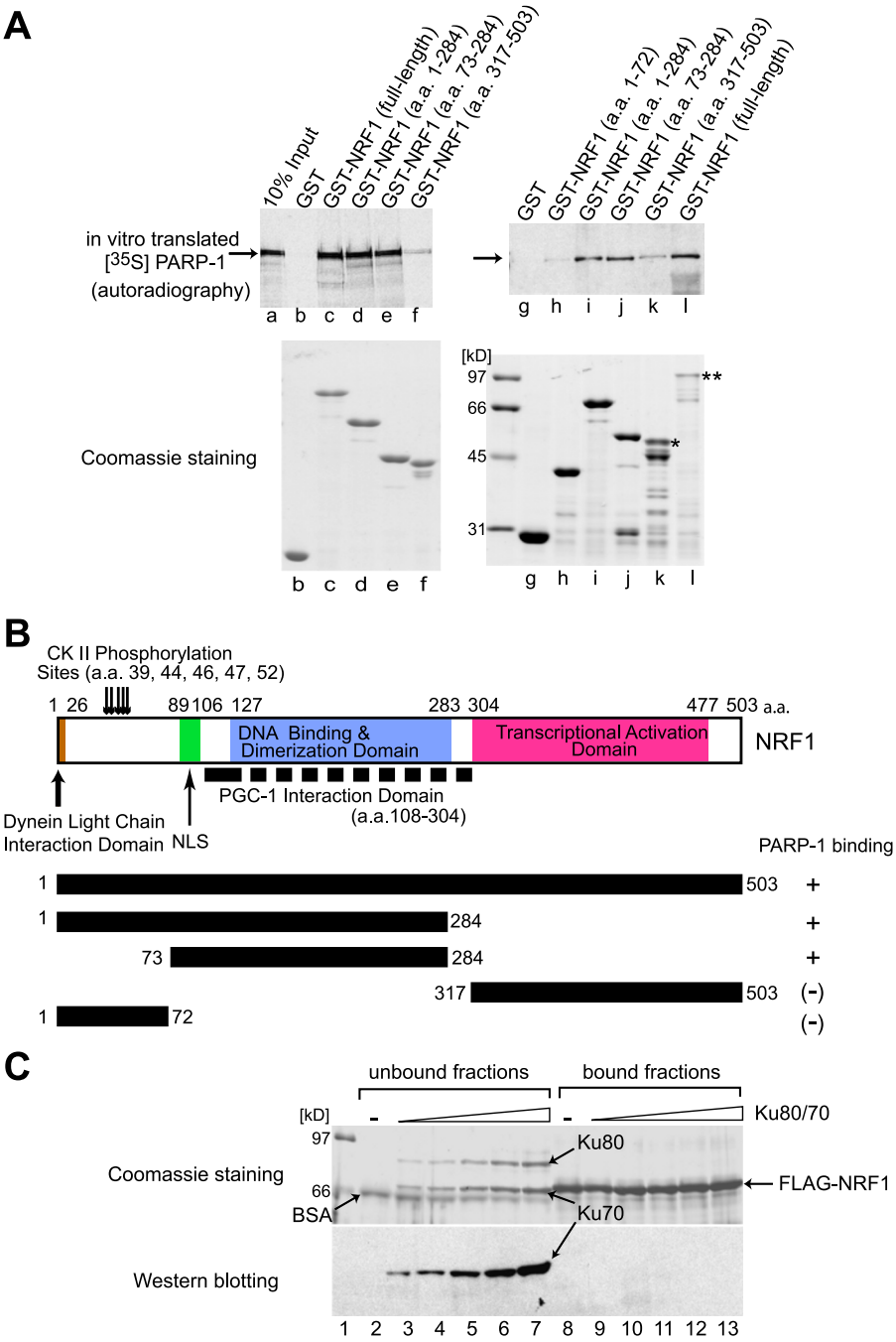

FIGURE 2. **PARP-1 directly binds to the DNA-binding/dimerization domain of NRF-1.** *A*, shown is the interaction between *in vitro* translated PARP-1 and bacterially expressed GST-fused NRF-1 proteins. GST-fused forms of full-length and different parts of NRF-1 protein were expressed in *E. coli* and purified with Glutathione-Sepharose. Purified GST-NRF-1 proteins (on beads) were incubated with full-length untagged PARP-1, which was *in vitro* translated in the presence of [^{35}S]methionine using rabbit reticulocyte lysate (TNT system). After incubation, the beads were washed several times, and the bound fractions were separated by SDS-PAGE and visualized by autoradiography. The *two upper panels* (*lanes a–f* and *g–l*) show ^{35}S autoradiography, and the *two lower panels* (*lanes b–f* and *g–l*) show Coomassie Blue-stained gels of the GST-NRF-1 proteins used for the binding assays. * and ** denote nonspecific proteins from *E. coli*. *B*, shown is a summary of the NRF-1-PARP-1 binding experiments. The region aa 73–284 that contains DNA-binding/dimerization domain of NRF-1 was found to interact with PARP-1. *C*, Ku80/Ku70 does not directly bind to NRF-1. Ku80 and Ku70 were co-expressed in SF9 cells, purified with Ni-NTA affinity beads, and eluted with imidazole, and then imidazole was removed by ultrafiltration. Increasing amounts of the purified Ku80/Ku70 complex were mixed with decreasing amount of bovine serum albumin to keep the protein concentration constant and then mixed with FLAG-NRF-1, which was immobilized on anti-FLAG(M2) beads. Unbound and bound fractions (after washing) were analyzed by SDS-PAGE followed by Coomassie Blue staining or anti-Ku70 Western blotting. *BSA*, bovine serum albumin.

subjected to mass spectrometry analyses as described under "Experimental Procedures." We found they were DNA-PK catalytic subunit, PARP-1, and Ku80. Because it was previously reported that DNA-PK, Ku80, Ku70, PARP-1, and TopoIIβ form a protein complex that plays a role in not only DNA repair but also transcriptional regulation (17–22), we were curious to see whether NRF-1 could co-purify all of the previously identified components of this complex. As shown in Fig. 1*B*, our anti-NRF-1 immunoprecipitation from crude nuclear extract followed by Western blotting using antibodies against various proteins confirmed that all of the known components of the complex, DNA-PK, TopoIIβ, PARP-1, Ku80, and Ku70, could be co-purified with NRF-1.

The DNA-binding/Dimerization Domain of NRF-1 Directly Interacts with the N-terminal Half of PARP-1—Next, we investigated which protein in the complex directly interacts with NRF-1. Because the PARP-1 signals from our pull-down experiments were consistently the strongest among the three co-purified proteins (Fig. 1*A*), we first examined whether PARP-1 could directly interact with NRF-1. *In vitro* translated ^{35}S-labeled full-length PARP-1 was incubated with bacterially expressed GST-fused full-length NRF-1. As shown in Fig. 2*A* (*lanes c* and *l*, *top panels*), specific binding of PARP-1 with NRF-1 was observed. We also carried out binding experiments using several NRF-1 deletion mutants. We found that the DNA-binding/dimerization domain (aa 73–284; Fig. 2*A*, *lanes e* and *j*) contained the major portion of PARP-1-binding region, whereas the N-terminal region (aa 1–72, *lane h*) and the C-terminal transcriptional activation domain (aa 317–503, *lanes f* and *k*) showed a marginal or background level of binding to PARP-1 (see Fig. 2*B* for summary). We also examined whether Ku80/Ku70 could directly interact with NRF-1, but no significant interaction was detected (Fig. 2*C*).

To determine which PARP-1 domain(s) interacts with NRF-1, deletion mutants of PARP-1 were baculovirally expressed, and the crude extracts from the infected SF9 cells were incubated with purified and immobilized FLAG-NRF-1. We found that the N-terminal 524 amino acids of PARP-1 contained almost as strong of an NRF-1 binding activity as the full-length PARP-1 (Fig. 3*A*, *right top panel* for silver staining and *right lower panel* for anti-PARP-1 Western blotting, *lane 4 versus lane 8*). We also observed weak binding of smaller N-terminal regions (aa 1–235 and 1–370) by silver staining (Fig. 3*A*, *top right panel*, *lanes 2* and *3*, shown by *red stars*). This binding was also detected by Western blotting after a long exposure (supplemental Fig. S1), but the signal was very weak because our anti-PARP-1 antibody can recognize the N-terminal part of PARP-1 only weakly.

To examine the NRF-1 binding properties of PARP-1 more clearly, we made an additional series of PARP-1 mutant constructs. These PARP-1 mutant proteins were bacterially expressed in GST-fused or CBP-fused forms and affinity purified. The NRF-1 DNA-binding domain (aa 73–284) was also bacterially expressed and purified to homogeneity. The purified PARP-1 proteins on beads were mixed with the purified NRF-1 DNA-binding domain. After incubation, the beads were washed, and the bound fractions were examined for the presence of NRF-1 by Coomassie Blue staining (Fig. 3*B*, *upper panel*) and by anti-NRF-1 Western blotting (Fig. 3*B*, *lower panel*). We found that five PARP-1 mutants containing aa 1–224, 1–386, 1–486, 1–650, and 103–650 showed specific NRF-1 binding activity (*lanes 2–5* and *8*) but that aa 1–650 showed significantly stronger binding than the other four mutants. These results, taken together with the results from the experiments shown in Fig. 3*A*, suggest that the N-terminal half of PARP-1 (aa 1–524) is necessary and sufficient for the full-strength interaction with NRF-1, as summarized in Fig. 3*C*.

In addition, the results shown in Fig. 3 indicate that several small regions combined but not one short stretch of amino acids alone within the N-terminal 524 amino acids are involved in the interaction with NRF-1: 1) the region aa 1–103 appears to be involved because aa 103–650 showed reduced NRF-1 binding compared with aa 1–650 (Fig. 3*B*, *lane 5 versus lane 8*, see both *upper* and *lower panels*), but aa 1–93 is not sufficient for this binding (*lane 1*); 2) the region aa 103–225 or 93–224 appears to contain a critical region, because aa 103–650 binds to NRF-1 but aa 225–650 does not (Fig. 3*B*, *lane 7 versus lane 8*) and because aa 1–224 binds to NRF-1 but aa 1–93 does not (Fig. 3*B*, *lane 1 versus lane 2*); and 3) the region aa 486–524 also appears to contribute to NRF-1-binding because aa 1–486 shows clearly reduced NRF-1-binding compared with aa 1–524 (Fig. 3*B*, *lane 4 versus lane 5*). One possible explanation may be that there is a critical region for NRF-1 binding between amino acid 103 and 224 but for full-strength binding, additional regions (aa 1–103 and 486–524) are required. These regions may be involved in direct contact with NRF-1 or may be required to maintain overall conformation of PARP-1 protein. To understand the NRF-1·PARP-1 interaction more precisely, more extensive deletion/point mutation analysis of each protein and/or structural biological studies will be required.

NRF-1 Can Bind DNA and PARP-1 Simultaneously—Because NRF-1 uses its DNA-binding/dimerization domain for PARP-1 binding, we were curious to see whether NRF-1 could bind to the DNA and PARP-1 simultaneously. To address this question, we carried out EMSA using the HBV X promoter DNA and the purified NRF-1 and PARP-1 proteins. As shown in Fig. 4, the electrophoretic mobility of the DNA·NRF-1 complex was slightly shifted by the addition of PARP-1 (Fig. 4, *lanes 3 versus lane 6*), indicating that a DNA·NRF-1·PARP-1 complex was formed. When anti-PARP-1 was added to the DNA·NRF-1·PARP-1 mixture, the DNA·NRF-1·PARP-1 band was further shifted (Fig. 4, *lanes 6 versus lane 7*), confirming that the band in *lane 6* contained PARP-1. When anti-NRF-1 was added to DNA·NRF-1·PARP-1 mixture, the signal of NRF-1·PARP-1·DNA disappeared (Fig. 4, *lane 6 versus lane 8*), indicating that the band in *lane 6* reflects DNA·NRF-1·PARP-1 complex where NRF-1 was the primary contact with the DNA, but the *band* in *lane 6* was not a DNA·PARP-1 complex.

It has been shown that PARP-1 binds double-stranded DNA ends in a sequence-nonspecific manner (23). In our EMSA, the sequence-nonspecific PARP-1·DNA complexes were detected at the origin of the gel (Fig. 4, *lane 2*) partly because the PARP-1 (aa 1–650) is basic (pI = 9.14) and does not have much negative charge under the experimental conditions. When anti-PARP-1 antibody was added to the PARP-1·DNA mixture, the signal of the PARP-1·DNA complex became partially smeared between the origin and the high molecular weight range in the gel (*lane 4*), presumably because the interactions between PARP-1 and the DNA ends were partially inhibited and/or the conformation of the PARP-1·DNA complex was changed by binding of the anti-PARP-1 antibody to the PARP-1·DNA complex. When NRF-1, PARP-1, and the DNA are mixed (*lane 6*), some PARP-1 molecules were bound to the DNA through interaction with NRF-1 (marked with an *arrow* and labeled as *DNA·NRF-1·PARP-1* in Fig. 4), but other PARP-1 molecules were bound to the ends of the probe DNA (the signal of this PARP-1·DNA complex is seen at the origin of the gel).

The exact reason why DNA·NRF-1·PARP-1·anti-PARP-1 band (*lane 7*) was stronger than DNA·NRF-1·PARP-1 band (*lane 6*) is not clear. However, the interaction between PARP-1 and anti-PARP-1 described above might have made PARP-1 molecules more accessible to NRF-1 and also made more DNA molecules available for the sequence-specific NRF-1 binding, but anti-PARP-1 did not inhibit PARP-1·NRF-1 interaction. Taken together, our EMSA results suggest that a DNA·NRF-1·PARP-1 complex can be formed; hence NRF-1 can likely recruit PARP-1 to the NRF-1-binding DNA site at the promoter.

NRF-1·PARP-1 Interaction Is Independent of PARP-1 Auto-PARylation—It has been reported that PARP-1 interacts with a subunit of the transcription factor NFκB, p50, and inhibits the binding of NFκB to its DNA. However, when PARP-1 is auto-PARylated, PARP-1/NFκB interaction is disrupted, and the NFκB-DNA interaction becomes facilitated (24). In contrast, the interaction between PARP-1 and the transcription factor AP2 is not affected by PARP-1 auto-PARylation, but PARP-1 PARylates AP2, and this modification affects AP2 DNA binding (25). In the case of interaction between PARP-1

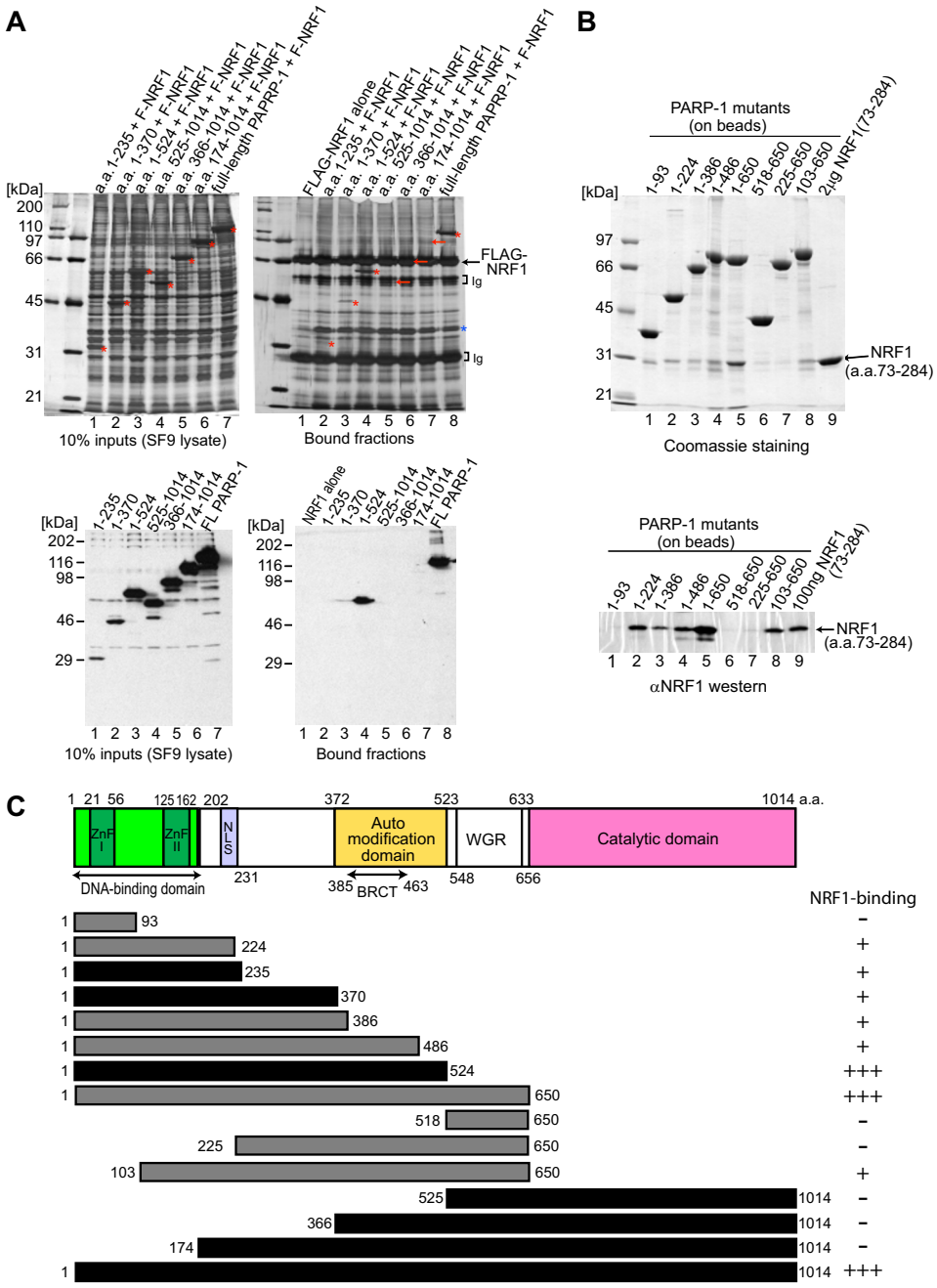

FIGURE 3. **N-terminal part of PARP-1 interacts with NRF-1.** *A*, binding assays using immobilized FLAG-NRF-1 and crude SF9 lysate containing baculovirally expressed PARP-1 proteins. *Upper left panel* shows silver staining of 10% inputs (crude SF9 lysate) used for the binding assays. The *red stars* show the expressed PARP-1 proteins. *Lower left panel* shows anti-PARP-1 Western analysis of the 10% inputs, confirming PARP-1 protein expression and checking reactivity of the mutant PARP-1 proteins to the anti-PARP-1 antibody. The *upper right panel* shows silver staining analysis of the bound fractions. The *red stars* show the PARP-1 proteins that were bound to FLAG-NRF-1/M2 beads, and the *red arrows* show the expected positions of some of the PARP-1 deletion mutants if they bound to NRF-1. Staining was extensively done to maximally detect the PARP-1 proteins. The *brackets* show the immunoglobulin (*Ig*) heavy chain (~55 kDa) and light chain (~28 kDa) derived from the M2 beads. The *lower right panel* shows anti-PARP-1 Western analysis of the bound fractions. Longer exposure of this Western blot is provided in the supplemental Fig. S1 to observe signals of 1–235 and 1–370. *B*, binding assays using purified and immobilized PARP-1 proteins and purified untagged NRF-1 DNA-binding domain. All of the PARP-1 proteins except the full-length synthetic PARP-1 (aa 1–650) were expressed in *E. coli* as GST fusion forms. The full-length synthetic PARP-1 was expressed in *E. coli* as a CBP fusion (see "Experimental Procedures"). ~2 μg of PARP-1 proteins on beads were incubated with ~20 μg of NRF-1 DNA-binding domain (aa 73–284) in a 100-μl reaction containing 20 mM Tris (pH 7.9), 200 mM NaCl, 10% glycerol, 2 mM $MgCl_2$, 2 μM $ZnCl_2$. The *upper panel* shows Coomassie staining of the bound fractions (*lanes 1–8*) and 2 μg of the purified NRF-1 DNA-binding domain (*lane 9*, as the size reference). The position of the NRF-1 (aa 73–284, ~31 kDa in SDS-PAGE) is shown by an *arrow*. The ~30-kDa protein in *lane 1* is a protein that co-purified with the GST-PARP-1 (aa 1–93) protein from *E. coli* but not NRF-1. The *lower panel* shows anti-NRF-1 Western blotting analyses of the bound fractions and the NRF-1 DNA-binding domain as a positive control. *C*, schematic of the PARP-1 deletion mutants used for binding assays and a summary of the NRF-1 binding experiments. The domain structure of the PARP-1 (1014 amino acids) is shown at the *top*. Previously identified domains and motifs shown are zinc fingers (*ZnF*), nuclear localization signal (*NLS*), BRCA1 C terminus domain (*BRCT*), WGR domain, and the PARP-1 catalytic domain (17, 18). Bacterially expressed PARP-1 proteins are shown in *gray*, and baculovirally expressed PARP-1 proteins are shown in *black*.

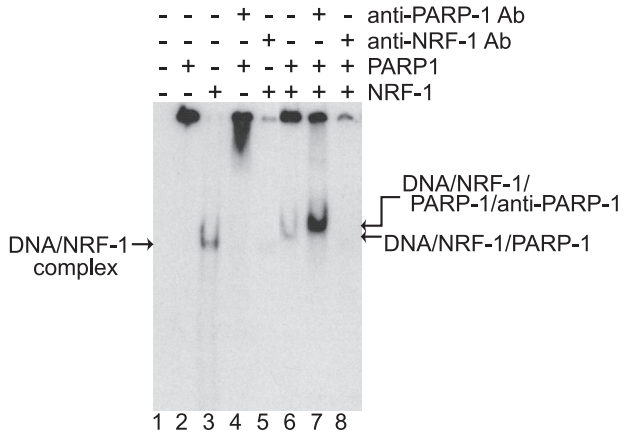

FIGURE 4. **NRF-1 can interact with DNA and PARP-1 simultaneously.** Indicated combinations of NRF-1 (full-length, no tag, purified), PARP-1 (aa 1–650, CBP fusion, purified), affinity-purified anti-PARP-1, and anti-NRF-1 were mixed with a ^{32}P-labeled 16-bp HBV DNA fragment containing the NRF-1-binding site. EMSA was performed as described under "Experimental Procedures."

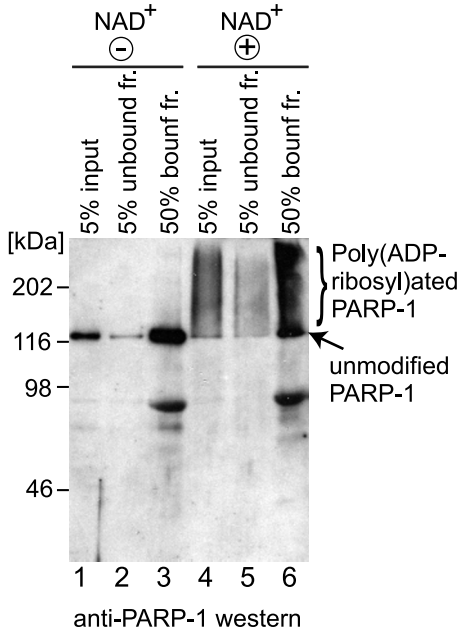

FIGURE 5. **PARylation of PARP-1 does not change NRF-1 binding activity of PARP-1.** Unmodified or auto-PARylated PARP-1 were prepared as described under "Experimental Procedures" and mixed with FLAG-NRF-1 on M2 beads. *Lanes 1–3* show analyses of binding with unmodified PARP-1, and *lanes 4–6* show analyses of PARylated PARP-1.

and the transcriptional co-activator mediator, PARP-1 catalytic activity is not required (21). Therefore, we wanted to know whether PARylation of PARP-1 or NRF-1 has any effect on the NRF-1·PARP-1 interaction. First, we purified a full-length PARP-1, auto-PARylated as described under "Experimental Procedures" and then tested its NRF-1 binding activity (Fig. 5, *lanes 4–6*). As a control, PARylation reaction was also carried out without NAD^+, and the resultant unmodified PARP-1 was used for the NRF-1-binding assay (Fig. 5, *lanes 1–3*). We found that the auto-PARylated PARP-1 as well as unmodified PARP-1 was able to bind NRF-1. Therefore, our results suggest that auto-PARylation of PARP-1 does not affect its NRF-1 binding activity.

PARP-1 PARylates NRF-1 and Modulates PARP-1·NRF-1 Interaction—To test whether NRF-1 could be PARylated by PARP-1, purified NRF-1 and PARP-1 proteins (shown in Fig. 6*A*) were incubated in a PARylation buffer and were examined for PARylation by Western blotting using an anti-PAR antibody. To monitor the level of PARP-1 auto-modification, PARylation reactions with PARP-1 alone were carried out in parallel. From these control reactions, PAR signals from only auto-modified PARP-1 with molecular weights higher than unmodified PARP-1 were detected (Fig. 6*B*, *lanes 2*, *6*, and *7*). No PAR signal was detected from the NRF-1 alone reaction (Fig. 6*B*, *lane 1*). From the NRF-1+PARP-1 reactions (Fig. 6*B*, *lanes 3*, *8*, and *9*), additional PAR signals compared with PARP-1 alone (*lanes 2*, *6*, and *7*) were detected. These additional signals (~80–120 or 80–150 kDa, shown with *brackets*) likely reflect PARylation of NRF-1. For positive controls, PARylation reactions were performed using known PARP-1 targets, p53, and histones (Fig. 6*B*, *lanes 4*, *5*, *16*, and *17*). We also carried out PARylation reactions using several other proteins including the DNA-binding domain of NRF-1 (aa 73–284) and as controls the general transcription factors TBP and TFIIB. We found that the DNA-binding domain of NRF-1 could be PARylated by PARP-1 (*lanes 10–11*), that TBP could be very efficiently PARylated (*lanes 12–13*), but that little or no TFIIB PARylation was detected (*lanes 14–15*). These results suggest that NRF-1 can be specifically PARylated by PARP-1, although it may not be as efficiently modified as p53 or histones, and that the DNA-binding domain of NRF-1 contains PARylation site(s). The isolated DNA-binding domain of NRF-1 may be PARylated by PARP-1 more efficiently than full-length NRF-1, but this issue will be addressed in the future.

Next, we asked whether PARylation of NRF-1 has any effect on the NRF-1·PARP-1 interaction. For this purpose, NRF-1 proteins were PARylated with PARP-1, and their PARP-1 binding activity was examined by following their PAR signals. As controls, PARylation reactions were performed without NAD^+, and PARP-1 binding of the unmodified NRF-1 proteins was monitored by anti-NRF-1 Western blotting. We found that both of the NRF-1 proteins (full-length or aa 73–384) could bind to PARP-1 after PARylation (Fig. 6*C*, *lanes 2* and *3*, shown with brackets), but their binding efficiency was very low, *i.e.* 50% of the PARP-1-bound fractions showed much weaker PAR signals of NRF-1 than 2% of unbound fractions (Fig. 6*C*, *lane 2 versus lane 5* for full-length NRF-1; and *lane 3 versus lane 6* of the shorter exposure for aa 73–284). In the control experiment, 50% of the PARP-1-bound fractions showed levels of NRF-1 signals approximately comparable with those of 2% unbound fractions (Fig. 6*C*, *lane 7 versus lane 9* for full-length NRF-1, *lane 8 versus lane 10* for aa 73–284). Thus, PARP-1 binding activity of NRF-1 appears to be reduced when NRF-1 is PARylated.

To further test whether NRF-1 PARylation modulates the NRF-1·PARP-1 interaction, we carried out another experiment. The NRF-1 protein (aa 73–284) was PARylated in the context of purified PARP-1·NRF-1 complex and then examined to see whether NRF-1 dissociated from PARP-1 after PARylation. GST-PARP-1·NRF-1 complexes were formed on glutathione-Sepharose beads, and PARylation reactions were carried out on

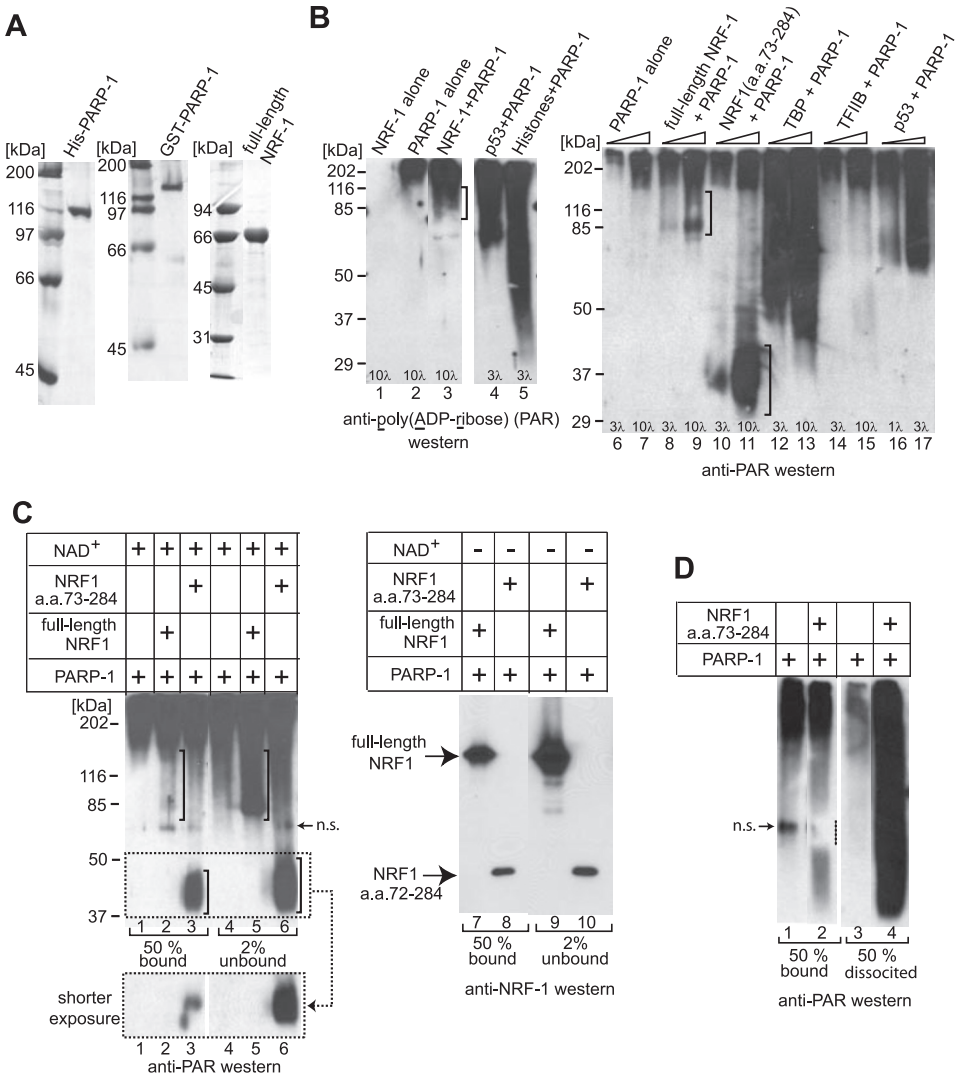

FIGURE 6. **PARP-1 PARylates NRF-1 and modulates PARP-1·NRF-1 interaction.** *A*, purified PARP-1 and NRF-1 proteins used in the PARylation experiments. The *left panel* shows silver staining analysis of the purified His-PARP-1 (full-length). The *central* panel shows silver staining analysis of the purified GST-PARP-1 (full-length). The *right panel* shows Coomassie Blue staining analysis of the purified full-length no tag NRF-1. SDS-PAGE analysis of NRF-1 DNA-binding domain (aa 73–284) is shown Fig. 3*B* (*lane 9*). *B*, NRF-1 can be PARylated by PARP-1. PARylation reactions of various proteins were performed as described under "Experimental Procedures" and then analyzed by anti-PAR antibody. The *brackets* show the positions of PARylated NRF-1 proteins (*lanes 3*, *8*, *9*, *10*, and *11*). Experiments with known PARylation targets, p53 and histones, were also performed as positive controls (*lanes 4*, *5*, *16*, and *17*). Because PARylation of p53 and histones were highly efficient, smaller volumes (1 and 3 μl) than NRF-1·PARP-1 reactions (3 and 10 μl) were loaded on the gel. *C*, PARylation of NRF-1 modulates PARP-1·NRF-1 interaction. 400 ng of NRF-1 proteins (full-length or aa 73–284) were incubated with GST-PARP-1 (40 ng) as described in *B* in the presence (*left panel*) or absence (*right panel*) of NAD^+ and then mixed with 2 μg of unmodified GST-PARP-1 and 3–4 μl of glutathione-Sepharose beads for 2 h at 4 °C. After the incubation, the beads were spun down, and supernatants (unbound fractions) were directly analyzed by Western blotting with either anti-PAR (*left panel*) or anti-NRF-1 antibody (*right panel*). The beads were analyzed by Western blotting after washing three times. Signals of nonspecific (*n.s.*) contaminants are indicated with an *arrow*. *D*, PARP-1·NRF-1 complex dissociates after NRF-1 PARylation. Glutathione-Sepharose beads (3–4 μl), GST-PARP-1 (2 μg), and full-length NRF-1 (800 ng) or NRF-1 (aa 73–284) (400 ng) were mixed together (30 μl volume) for 2 h at 4 °C. Then the beads were spun-down and washed once to remove unbound fraction. Next the washed beads were incubated in 20 μl of the complete PARylation buffer at room temperature for 40 min with occasional mixing, and then bead-bound and unbound (dissociated) fractions were analyzed by anti-PAR Western blotting. The *dotted line* by the *second lane* shows the position where proteins were not transferred efficiently because of an air bubble during the electroblotting. The *arrow* and *n.s.* show a signal from a non-specific contaminant.

beads. After the reaction, bead-bound fractions and unbound fractions were separated by centrifugation and were examined by anti-PAR Western blotting. As shown in Fig. 6*D*, the majority of the PARylated NRF-1 was detected in the unbound fraction (Fig. 6*D*, *lane 2 versus lane 4*), whereas the majority of the GST-PARP-1 was still bound to the glutathione beads (Fig. 6*D*, *lanes 1* and *2 versus lane 3*). Therefore, the signal observed in *lane 4* was likely due to dissociation of NRF-1 from PARP-1 but not dissociation of the NRF-1·PARP-1 complex from the glutathione beads. This dissociation is most likely due to NRF-1 modification but not PARP-1 auto-PARylation because we have shown in Fig. 5 that PARP-1 auto-PARylation does not change its NRF-1 binding activity. These results indicate that PARylated NRF-1 can still bind to PARP-1 but to a much lesser extent compared with unmodified NRF-1. Therefore, PARylation of NRF-1 may modulate the NRF-1·PARP-1 interaction.

PARP-1 Plays a Role in Transcriptional Activation by NRF-1—To study the functional contribution of PARP-1 in NRF-1 transcriptional activation, we examined effects of the overexpression or knock-down of PARP-1 and NRF-1. First, overexpression plasmids for NRF-1 and/or PARP-1 were transfected into HepG2 cells with a reporter plasmid that is driven by the HBV X gene start site 1 core promoter, which contains only an NRF-1-binding site and the core promoter element XCPE1. As shown in Fig. 7*A*, NRF-1 overexpression resulted in 2–3-fold activation of the X gene core promoter 1 as previously observed (13). Overexpression of PARP-1 resulted in only slight but consistent activation of the X gene core promoter 1. The absence of strong activation by overexpression of PARP-1 was likely due to the relatively high level of endogenous PARP-1 in HepG2 cells. Further activation of the X gene transcription was observed by co-overexpression of NRF-1 and PARP-1. These results indicate that NRF-1 and PARP-1 can cooperate with each other to bring about transcriptional activation of the X gene. To further evaluate our results from overexpression experiments, we next conducted siRNA knock-down experiments. HepG2 cells were transfected with NRF-1 and PARP-1 siRNAs individually or together along with the X gene core promoter 1 reporter construct. The effects of siRNAs on NRF-1 or PARP-1 mRNA expression were checked by RT-

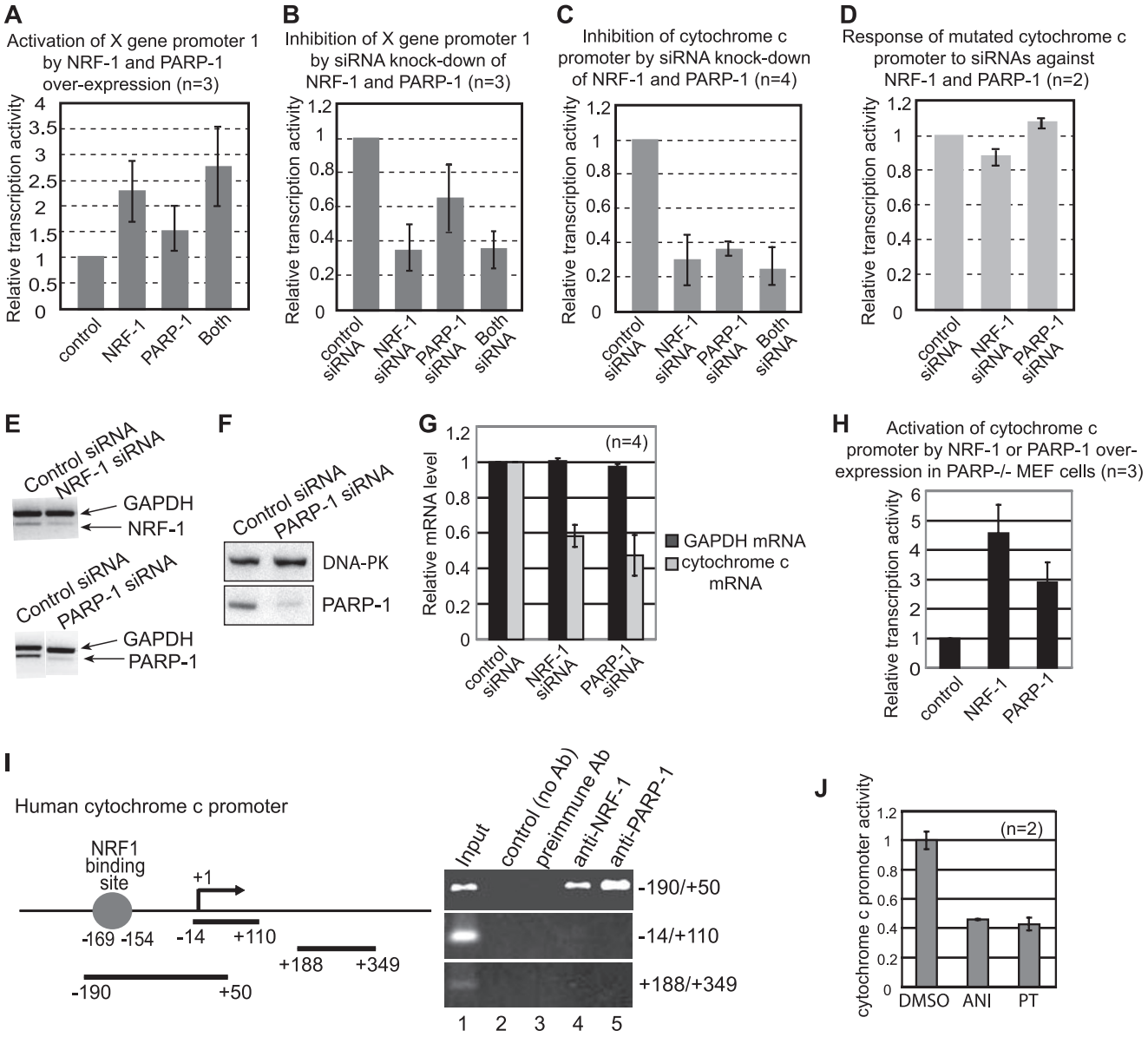

FIGURE 7. **PARP-1 plays a role in transcription activation by NRF-1.** *A*, overexpression of NRF-1 and/or PARP-1 activated transcription of the HBV X gene promoter. HepG2 cells were transfected with a firefly luciferase reporter plasmid driven by the minimal promoter of HBV X start site 1 with an NRF-1 overexpression plasmid and/or a PAPR-1 overexpression plasmid as described under "Experimental Procedures." Standard errors are shown by *bracketed bars* on the bar graph. The graphs in *B–D*, *G*, *H*, and *J* also show S.E. *B*, HepG2 cells were transfected with the same reporter plasmid but with siRNAs targeting NRF-1 and/or PARP-1. *C*, HepG2 cells were transfected with the siRNAs targeting NRF-1 and/or PARP-1 two times and then with a luciferase reporter plasmid driven by human cytochrome C promoter plus the siRNAs targeting NRF-1 and/or PARP-1. *D*, HepG2 cells were transfected with the siRNAs targeting NRF-1 or PARP-1 two times and then with the luciferase reporter plasmid driven by cytochrome *c* promoter containing mutated NRF-1-binding site plus the siRNAs targeting NRF-1 or PARP-1. *E*, RT-PCR analyses of NRF-1 and PARP-1 expression after siRNA treatments. Glyceraldehyde-3-phosphate dehydrogenase (*GAPDH*) is a control whose expression was not affected by NRF-1 or PARP-1 siRNA. *F*, Western blot analysis of PARP-1 protein expression after the three times treatment with PARP-1 siRNA. Western blot analysis of DNA-PK was carried out in parallel as a control whose protein level was not changed after the PARP-1 siRNA treatments. *G*, quantitative RT-PCR analysis of endogenous cytochrome *c* mRNA. After NRF-1 or PARP-1 siRNA treatment, total RNA was extracted from the transfected HepG2 cells, and the levels of cytochrome *c* mRNA were measured by RT-PCR as described under "Experimental Procedures." Glyceraldehyde-3-phosphate dehydrogenase mRNA levels were monitored as an internal control. *H*, *PARP-1*$^{-/-}$ MEF cells were transfected with NRF-1 or PARP-1 overexpression plasmid with the reporter plasmid driven by the cytochrome *c* promoter. *I*, co-localization of NRF-1 and PARP-1 on the cytochrome *c* promoter. ChIP was performed using no antibody, preimmune, anti-NRF-1, or anti-PARP-1 antibody. A cytochrome *c* promoter region that contains the NRF-1-binding site (−190 to +50), and regions that do not contain NRF-1-binding site (−14 to +110 and +188 to +349) were amplified by PCR as described under "Experimental Procedures." *J*, PARP-1 inhibitors reduced cytochrome *c* gene transcription. HepG2 cells were transfected with cytochrome *c* reporter plasmid for 7 h and then treated with dimethyl sulfoxide (*DMSO*) alone (final 2.5%), 4-amino-1,8-naphthalimide (*ANI*) (20 μM), or 6(5H)-phenanthridinone (*PT*) (4 μM) overnight, and then the reporter activities were measured.

PCR (Fig. 7*E*). Transcriptional inhibition of the X gene promoter 1 was seen upon siRNA knock-down of PARP-1 and/or NRF-1 (Fig. 7*B*). We noticed that inhibition by PARP-1 siRNA was not very strong, which may be again in part reflection of the high level of endogenous PARP-1, *i.e.* even if the PARP-1 levels reduced significantly by siRNA treatment, there might be still sufficient PARP-1 remaining in the cells to support transcriptional activation by NRF-1, resulting in only a small inhibition. The effect of PARP-1 siRNA on PARP-1 protein level was also examined by Western blotting to confirm that PARP-1 siRNA

was functioning, after transfection three times of PARP-1 siRNA (Fig. 7*F*). This point will be further discussed under "Discussion."

We also observed similar effects on transcription from the human somatic cytochrome *c* promoter (Fig. 7*C*), a known NRF-1 target promoter (26). To further determine whether inhibition of cytochrome *c* transcription by the siRNA treatments were through the NRF-1-binding site, we constructed another cytochrome *c* reporter plasmid whose NRF-1-binding site is mutated. Transcription from this mutated cytochrome *c* reporter plasmid was not changed by the siRNAs (Fig. 7*D*); thus NRF-1 and PARP-1 appear to activate transcription of cytochrome *c* gene mainly through the NRF-1-binding site. We also found that the level of endogenous cytochrome *c* mRNA was reduced by NRF-1 or PARP-1 siRNA treatment (Fig. 7*G*). Transfection of *PARP-1*$^{-/-}$ MEF cells with NRF-1 and PARP-1 overexpression plasmids showed activation of the cytochrome *c* promoter (Fig. 7*H*).

To investigate whether NRF-1 and PARP-1 are co-localized at the cytochrome *c* promoter, ChIP experiments were conducted. We found that both anti-NRF-1 and anti-PARP-1 chromatin immunoprecipitates contained the cytochrome *c* promoter region (−190 to +50) that contained the NRF-1-binding site, but not the downstream regions (−14 to +110 or +188 to +349) (Fig. 7*I*, *lanes 4* and *5*). In contrast, control ChIP precipitated neither region of cytochrome *c* promoter (Fig. 7*I*, *lanes 2* and *3*). These results suggest that NRF-1 and PARP-1 are co-localized at the NRF-1-binding site of the human cytochrome *c* promoter.

To test whether PARP-1 enzymatic activity is important for NRF-1 transcriptional activation, the cytochrome *c* reporter plasmid was transfected into HepG2 cells, and then the cells were treated with PARP-1 inhibitors 4-amino-1,8-naphthalimide and 6(5H)-phenanthridinone (27, 28). As shown in Fig. 7*J*, we observed reduction of cytochrome *c* promoter activity when cells were treated with the PARP-1 inhibitors. Taken together, these results are consistent with the idea that PARP-1 contributes significantly in transcriptional activation by NRF-1.

DISCUSSION

PARP-1 Interacts with NRF-1 and Is Involved in NRF-1 Transcriptional Regulation—To better understand the mechanisms of transcriptional activation by NRF-1, we screened nuclear extracts for NRF-1-interacting proteins and found that NRF-1 could interact with PARP-1 directly. We also found that NRF-1 could pull down the PARP-1·DNA-PK·Ku80·Ku70·TopoIIβ-containing complex through interactions with at least PARP-1, but not Ku80 or Ku70. Our EMSA assays showed that the NRF-1-PARP-1 interaction could occur while NRF-1 was bound to the promoter DNA, so NRF-1 may be able to recruit the PARP-1·DNA-PK·Ku80·Ku70·TopoIIβ-containing complex to the NRF-1 target promoters. This observation was further supported by our ChIP assay, showing that NRF-1 and PARP-1 co-localized at the cytochrome *c* promoter region that contains an NRF-1-binding site. Our transfection experiments of overexpression or siRNA knock-down of PARP-1 and NRF-1 suggested that the interaction between PARP-1 and NRF-1 is functionally important in transcriptional activation by NRF-1. Our experiments with PARP-1 inhibitors suggested that PARP-1 enzymatic activity is used during NRF-1 transcriptional activation. Our *in vitro* experiments showed that PARP-1 could specifically PARylate NRF-1, and one or more PARylation site(s) was located in the NRF-1 DNA-binding domain aa 73–284. This NRF-1 modification by PARP-1 appeared to modulate interaction between NRF-1 and PARP-1, whereas auto-PARylation of PARP-1 did not change the NRF-1·PARP-1 interaction.

In the future, it will be interesting to address the following issues: 1) interrelation among NRF-1 PARylation, NRF-1 N-terminal phosphorylation by casein kinase II (29), and NRF-1 phosphorylation by DNA-PK[3]; 2) whether NRF-1 DNA binding activity is regulated by such modifications; 3) whether DNA-PK, Ku80/70, and TopoIIβ are also co-localized at NRF-1 target promoters; 4) which PARylation target(s) of PARP-1 actually play a critical role in transcriptional activation by NRF-1 (because PARP-1 has been shown to PARylate histones and many other transcription factors (17)); and 5) whether PARylation of PARP-1 can change composition of the NRF-1-bound PARP-1·DNA-PK·Ku·TopoIIβ-containing complex.

Relationship between the PARP-1·DNA-PK·Ku80·Ku70·TopoIIβ Complex and PGC-1 Family Members in NRF-1 Transcriptional Activation—Because PGC-1α, PGC-1β, and PRC have been shown to interact with NRF-1, in our pull-down experiments we had expected that PGC-1 family members might be co-purified with NRF-1, in addition to novel interacting partners (Fig. 1*A*). However, we detected only DNA-PK, PARP-1, and Ku80. The reason our pull-down reaction did not show PGC-1 family members is unclear. However, it may reflect the relatively low steady state level of protein concentrations for PGC-1 family members in the nuclear extracts we used compared with concentrations of PARP-1. PGC-1α and PGC-1β are known to be expressed in both tissue-specific and inducible manners (5, 30), and PRC has been shown to be expressed in a cell cycle phase-specific manner (G_0-to-G_1 transition or immediate early phase). PRC protein is also known to be very unstable (30). In fact, we could actually detect an interaction between NRF-1 and PGC-1α when we mixed *in vitro*-translated PGC-1α and baculovirally expressed NRF-1 *in vitro*.[4] Thus, our observations are consistent with previously reported observations about NRF-1 and PGC-1 family members but provide additional information regarding activation by NRF-1. It is possible that PARP-1 plays a major role in co-activating NRF-1 when levels of PGC-1 family members are not very high in cells to maintain the basal level of NRF-1-target gene expression. However, it will be important to determine whether PARP-1 and PGC-1 family members compete with each other for NRF-1 binding or whether they can cooperate with each other to activate transcription because we found in this study that PARP-1 binds to the NRF-1 DNA-binding domain, which has been also shown to bind PGC-1α. *In vitro* binding competition experiments using PARP-1 and PGC-1α are underway.

The reason our first pull-down experiment (Fig. 1*A*) did not show Ku70 and TopoIIβ may be as follows. Because Ku70

[3] M. B. Hossain and S. Takada, unpublished results.
[4] R. Anish and S. Takada., unpublished data.

shows the same mobility as NRF-1 in SDS-PAGE, we could not observe the presence of Ku70 by silver staining, even though it actually co-purified. TopoIIβ may be relatively loosely associated with the rest of the PARP-1·DNA-PK complex, and this can explain why the association of TopoIIβ with the PARP-1·DNA-PK·Ku complex was found only recently (22). For the same reason, TopoIIβ might have fallen off from the complex during our extensive washing and the nuclease treatment of the pull-down reactions. Our anti-NRF-1 immunoprecipitation experiment shown in Fig. 1*B* and the observation by Ju *et al.* (22) together strongly suggest that NRF-1 can interact with the entire PARP-1·DNA-PK·Ku80·Ku70·TopoIIβ-containing complex.

Multiple Mechanisms of PARP-1 Function in NRF-1 Transcriptional Regulation?—Our NRF-1 and PARP-1 overexpression experiments and siRNA experiments suggest that the interaction between NRF-1 and the PARP-1 is functionally important. However, it is interesting to note that reduction of transcription from the NRF-1 target reporters did not appear to be as striking as the reduction of PARP-1 mRNA/protein levels. This may be simply because PARP-1 is so abundant in the cells that there was still enough PARP-1 after the siRNA treatment to co-activate NRF-1. However, transcriptional regulation by PARP-1 involves, at least in part, a histone H1-HMGB (high mobility group B) exchange event and/or depletion of histone H1 and concomitant replacement with PARP-1 that occurs in the context of chromatin (22, 31) and also likely involves PARylation of histones H1, H2A, H2B, H3, H4, and H5 (18, 32, 33). Therefore, in transient transfection experiments where reporter plasmids are not likely to have complete chromatin structures, this component of the PARP-1 function may not be readily detectable.

However, there is evidence that PARP-1 also has functions that can be observed without a complete chromatin context. First, PARP-1 had been identified as one of the general transcription co-factors TFIIC, which was required for site-specific initiation of transcription by RNA polymerase II when nicked and not chromatin assembled DNA templates were used for *in vitro* transcription assays (34, 35). Second, PARP-1 directly interacts with mediator and plays an essential role in switching the mediator complex from an inactive form (the large Cdk8-containing mediator complex) to an active form (Cdk8$^-$ mediator complex, CRSP (cofactor required for Sp1 activation), or PC2). This PARP-1 activity could be observed in *in vitro* transcription assays without chromatin templates (21, 36). Because our previous study (14) that identified the required factors for transcription from the HBV X minimal promoter revealed a requirement of NRF-1 and the mediator complex and because the mediator is known to directly interact with RNA polymerase II, NRF-1 may activate transcription by enhancing recruitment of RNA polymerase II to the promoter using a network of protein-protein interactions between NRF-1, PARP-1, mediator, and RNA polymerase II.

Another important possibility to be noted is that PARP-1 may play a dual role in transcriptional regulation with NRF-1, because PARP-1 has been shown to be involved in both transcriptional activation and repression (see Ref. 33 for review). For example, PARP-1 has been found to be a component of the nuclear receptor co-repressor or the *Groucho*/TLE1 co-repressor complex while target genes are uninduced but actually plays a critical role in the step of co-repressor-co-activator exchange upon activation of the promoters in response to signals or hormone stimulation (19, 22). During this event, PARP-1 is present in both the co-repressor and the co-activator complex. It is not known whether NRF-1 associates with co-repressor complex, but there is a report that NRF-1 could also be involved in transcriptional repression when it is glycosylated (37). Thus, there may be an additional level of regulation that makes the effect of PARP-1 siRNA more complicated. To gain a more detailed understanding of the molecular mechanisms for transcriptional activation by NRF-1, the roles of each component in the NRF-1-PARP-1 complex, their modification status, and the state of chromatin structure and histone modification of the transcription template need to be characterized.

Taken together, our data suggest that PARP-1 plays a role in transcriptional regulation by NRF-1. It will be interesting to find out the exact molecular events that occur at the promoter region that underlie transcriptional activation by NRF-1 and the PARP-1-containing complex. Our findings described here raise a number of interesting questions to address in the future, to further our understanding of transcriptional activation mechanisms for NRF-1 in the context of core promoters.

Acknowledgments—We thank Suparna Bhattacharya for protein purification of the NRF-1 DNA-binding domain, Zheng-Qing Wang and Kyoko Yokomori for PARP-1$^{-/-}$ MEF cells. We also thank Michelle Barton, Sabrina Stratton, Kendra Alton, and Joe Taube for advice to our ChIP experiments.

REFERENCES

1. Scarpulla, R. C. (2006) *J. Cell. Biochem.* **97,** 673–683
2. Scarpulla, R. C. (2008) *Physiol. Rev.* **88,** 611–638
3. Virbasius, C. A., Virbasius, J. V., and Scarpulla, R. C. (1993) *Genes Dev.* **7,** 2431–2445
4. Xi, H., Yu, Y., Fu, Y., Foley, J., Halees, A., and Weng, Z. (2007) *Genome Res.* **17,** 798–806
5. Andersson, U., and Scarpulla, R. C. (2001) *Mol. Cell. Biol.* **21,** 3738–3749
6. Wu, Z., Puigserver, P., Andersson, U., Zhang, C., Adelmant, G., Mootha, V., Troy, A., Cinti, S., Lowell, B., Scarpulla, R. C., and Spiegelman, B. M. (1999) *Cell* **98,** 115–124
7. Lin, J., Tarr, P. T., Yang, R., Rhee, J., Puigserver, P., Newgard, C. B., and Spiegelman, B. M. (2003) *J. Biol. Chem.* **278,** 30843–30848
8. Puigserver, P., Adelmant, G., Wu, Z., Fan, M., Xu, J., O'Malley, B., and Spiegelman, B. M. (1999) *Science* **286,** 1368–1371
9. Monsalve, M., Wu, Z., Adelmant, G., Puigserver, P., Fan, M., and Spiegelman, B. M. (2000) *Mol. Cell* **6,** 307–316
10. Wallberg, A. E., Yamamura, S., Malik, S., Spiegelman, B. M., and Roeder, R. G. (2003) *Mol. Cell* **12,** 1137–1149
11. Herzig, R. P., Andersson, U., and Scarpulla, R. C. (2000) *J. Cell Sci.* **113,** 4263–4273
12. Gugneja, S., Virbasius, C. M., and Scarpulla, R. C. (1996) *Mol. Cell. Biol.* **16,** 5708–5716
13. Tokusumi, Y., Zhou, S., and Takada, S. (2004) *J. Virol.* **78,** 10856–10864
14. Tokusumi, Y., Ma, Y., Song, X., Jacobson, R. H., and Takada, S. (2007) *Mol. Cell. Biol.* **27,** 1844–1858
15. Wang, Z. Q., Auer, B., Stingl, L., Berghammer, H., Haidacher, D., Schweiger, M., and Wagner, E. F. (1995) *Genes Dev.* **9,** 509–520
16. Zeng, P. Y., Vakoc, C. R., Chen, Z. C., Blobel, G. A., and Berger, S. L. (2006) *BioTechniques* **41,** 694–698
17. Aguilar-Quesada, R., Munoz-Gamez, J. A., Martin-Oliva, D., Peralta-Leal,

A., Quiles-Perez, R., Rodriguez-Vargas, J. M., de Almodovar, M. R., Conde, C., Ruiz-Extremera, A., and Oliver, F. J. (2007) *Curr. Med. Chem.* **14,** 1179–1187
18. Schreiber, V., Dantzer, F., Ame, J. C., and de Murcia, G. (2006) *Nat. Rev. Mol. Cell Biol.* **7,** 517–528
19. Ju, B. G., Solum, D., Song, E. J., Lee, K. J., Rose, D. W., Glass, C. K., and Rosenfeld, M. G. (2004) *Cell* **119,** 815–829
20. Kim, M. Y., Mauro, S., Gevry, N., Lis, J. T., and Kraus, W. L. (2004) *Cell* **119,** 803–814
21. Pavri, R., Lewis, B., Kim, T. K., Dilworth, F. J., Erdjument-Bromage, H., Tempst, P., de Murcia, G., Evans, R., Chambon, P., and Reinberg, D. (2005) *Mol. Cell* **18,** 83–96
22. Ju, B. G., Lunyak, V. V., Perissi, V., Garcia-Bassets, I., Rose, D. W., Glass, C. K., and Rosenfeld, M. G. (2006) *Science* **312,** 1798–1802
23. Kraus, W. L. (2008) *Curr. Opin. Cell Biol.* **20,** 294–302
24. Chang, W. J., and Alvarez-Gonzalez, R. (2001) *J. Biol. Chem.* **276,** 47664–47670
25. Li, M., Naidu, P., Yu, Y., Berger, N. A., and Kannan, P. (2004) *Biochem. J.* **382,** 323–329
26. Scarpulla, R. C. (2002) *Biochim. Biophys. Acta* **1576,** 1–14
27. Schlicker, A., Peschke, P., Burkle, A., Hahn, E. W., and Kim, J. H. (1999) *Int. J. Radiat. Biol.* **75,** 91–100
28. Banasik, M., Komura, H., Shimoyama, M., and Ueda, K. (1992) *J. Biol. Chem.* **267,** 1569–1575
29. Gugneja, S., and Scarpulla, R. C. (1997) *J. Biol. Chem.* **272,** 18732–18739
30. Kressler, D., Schreiber, S. N., Knutti, D., and Kralli, A. (2002) *J. Biol. Chem.* **277,** 13918–13925
31. Krishnakumar, R., Gamble, M. J., Frizzell, K. M., Berrocal, J. G., Kininis, M., and Kraus, W. L. (2008) *Science* **319,** 819–821
32. Ogata, N., Ueda, K., and Hayaishi, O. (1980) *J. Biol. Chem.* **255,** 7610–7615
33. Thomas, M. C., and Chiang, C. M. (2006) *Crit. Rev. Biochem. Mol. Biol.* **41,** 105–178
34. Slattery, E., Dignam, J. D., Matsui, T., and Roeder, R. G. (1983) *J. Biol. Chem.* **258,** 5955–5959
35. Meisterernst, M., Stelzer, G., and Roeder, R. G. (1997) *Proc. Natl. Acad. Sci. U. S. A.* **94,** 2261–2265
36. Malik, S., Guermah, M., Yuan, C. X., Wu, W., Yamamura, S., and Roeder, R. G. (2004) *Mol. Cell. Biol.* **24,** 8244–8254
37. Gomez-Cuadrado, A., Martin, M., Noel, M., and Ruiz-Carrillo, A. (1995) *Mol. Cell. Biol.* **15,** 6670–6685